TRANSPORTES
revistatransportes.org.br
anpet
associação nacional de pesquisa e ensino em transportes
anpet.org.br

Development of friction coefficient prediction models for Brazilian runways using Artificial Neural Networks

Desenvolvimento de modelos de previsão de coeficiente de atrito em pistas de pouso e decolagem brasileiras com Redes Neurais Artificiais

Túlio Rodrigues Ribeiro[1], **Francisco Heber Lacerda de Oliveira**[1]

[1]Federal University of Ceará, Fortaleza, Ceará, Brasil

Contact: tulio.rodrigues.r@hotmail.com (TRR); heber@det.ufc.br, (FHLO)

Submitted:
7 June, 2022
Accepted for publication:
17 March, 2023
Published:
31 August, 2023

Associate Editor
Kamilla Vasconcelos
Universidade de São Paulo, Brasil

Keywords:
Airfield pavements.
Skid resistance.
Coefficient of friction.
Operational safety.

Palavras-chave:
Pavimentos aeroportuários.
Resistência à derrapagem.
Coeficiente de atrito.
Segurança operacional.

DOI: 10.58922/transportes.v31i2.2792

ABSTRACT
Landing and takeoff procedures are the prior most critical phases of a flight, once they are up to several factors that play a fundamental role in its performance, these include the pilot´s skill, weather states and skid resistance. In this context, the friction coefficient represents an important parameter for operational safety in terms of tire-pavement adherence. In that fashion, this research aims to offer confident prediction models supported by Artificial Neural Networks as a way of quantifying friction coefficient based on 3-6 meters from the axis of runways (RWY) through different types of equipment in virtue of assisting the aerodrome operator with respect of safety procedural requirements, in addition to verifying the influence of grooving upon friction coefficient performance. The models developed have achieved some satisfactory results, given the complexity of the problem, emphasizing the significance of further improvements, even though these models might settle on ways that help guide and control RWY safety procedures.

RESUMO
As operações de pouso e decolagem representam as fases mais críticas de um voo, uma vez serem suscetíveis a diversos fatores que intervêm em seu desempenho, tais como a habilidade do piloto, as condições climáticas e de aderência pneu-pavimento. Nesse contexto, o coeficiente de atrito representa um parâmetro importante para a segurança operacional no quesito aderência pneu-pavimento. Dessa forma, esta pesquisa visa desenvolver modelos de previsão utilizando Redes Neurais Artificiais para o coeficiente de atrito medido a 3 e a 6 metros do eixo de pistas de pouso e decolagem (PPD) por meio de diferentes tipos de equipamento com a finalidade de auxiliar o operador de aeródromo quanto à garantia da segurança operacional, além de verificar a influência do *grooving* no desempenho do coeficiente de atrito. Os modelos desenvolvidos apresentaram resultados satisfatórios dada a complexidade do problema, demonstrando que, apesar de necessitar de aprimoramentos futuros, eles podem contribuir com a segurança das operações nas PPD.

1. INTRODUCTION

In the airport context, runways (RWY) become more requested as the flow of passengers and cargo grows, as well as the emergence of new operations with larger and heavier aircraft that contribute to the premature wear and tear of airport pavements. This increase may imply a greater number of accidents and aeronautical incidents, which have a greater occurrence and safety risk during ground operations (ICAO, 2019).

Shahin (2005) states that the relevance of preserving the texture of airport pavements is obvious since their poor condition can contribute to the occurrence of an incident or air accident. This is due, in many cases, to deficiencies in the coating, mainly with regard to the tire-pavement adherence parameters, namely, the friction coefficient and the macrotexture, which are also affected by the accumulation of rubber from the aircraft tires.

In addition to grip conditions, adversity in weather can result in contamination of the RWY by water, causing a negative impact on braking, acceleration and aircraft stability. The presence of water on the pavement surface is mainly attributed to its surface and drainage characteristics (ICAO, 2019).

It is understood, therefore, that the evaluation of tire-pavement adherence parameters is essential to ensure the safety of landing and takeoff operations. According to ANAC (2019), the number of parameter measurements is directly proportional to the number of operations at the RWY, and, for this reason, the RWY remains closed or partially blocked, restricting operations at the airport. Thus, the application of mathematical models capable of predicting the adherence conditions of the RWY coating is justified.

In view of the above, the technique of Artificial Neural Networks was used in order to develop models for predicting the friction coefficient obtained through reports of measurements in the field, carried out at the two Brazilian airports, between 2012 and 2018.

2. ASPECTS THAT INFLUENCE THE FRICTION COEFFICIENT

According to Fonseca (1990), the friction coefficient represents the effect of the macrotexture associated with the microtexture. The action of the surface texture on the friction coefficient of the RWY is subject to the speed developed by the aircraft and the effectiveness of the pavement drainage (Kazda and Caves, 2007). Among the factors that influence the friction coefficient stand out the type of pavement, surface texture, traffic and time, removal of rubber accumulation and climatic conditions. Aps (2006) found that the draining coating has a better performance for the coefficient of longitudinal friction and greater stability of friction in view of the development of speed. This is a consequence of the draining effect of surface water through the interconnected voids. However, the lowest values of longitudinal friction coefficient were evidenced in Asphaltic Concrete (AC), which is the most influenced by the increase in speed.

McDaniel et al. (2010) analyzed the behavior of the friction coefficient in certain segments of North American highways from the opening of the lanes to traffic up to a 5-years period, using the DFT equipment, at a speed of 20 km/h. Surfaces with Stone Matrix Asphalt (SMA) and Porous Friction Course showed stable and similar friction coefficient levels, however, significantly higher than the AC, even though the latter is in an acceptable condition. No consistent downward trend was perceived; after the action of the traffic, the stretch with AC presented the lowest friction values among the types of coatings analyzed.

Costa et al. (2017) investigated the variation of the friction coefficient in different paving techniques, using the British Pendulum equipment. It is observed that the AC with the addition of rubber had the lowest British Pendulum Number (BPN), presenting lower values than the AC, while the pavement with the presence of grooving obtained the highest BPN, that is, better skid resistance. However, when the rubbering component is included, there is a reduction of about one third of the BPN value. This is due to the process of filling the transverse grooves with rubber waste from vehicles tires wear.

Skerritt (1993) understands that the friction in new pavements comes mainly from the macrotexture, as the aggregates are still covered with an asphalt film. However, as vehicles travel along the road, this layer disappears, and the aggregates are exposed to polishing. In a given time, all surface aggregates wear down until they reach an equilibrium condition. This state is reached after passing 1 to 5 million passenger vehicles or after a period of two years. In fact, the geometry of the lane and the intensity of vehicle traffic, especially commercial vehicles, exert a direct influence on the polishing of the aggregates. Therefore, roads with high traffic volume demand more caution with friction (Chelliah et al., 2002).

Chen et al. (2008) analyzed the performance of the friction coefficient in relation to the effect of rubber accumulation in a RWY at Kaohsiung International Airport, in Taiwan. It was found that after the initial 200 m, with the beginning of the predominant headland, it is already possible to observe the presence of small rubber deposits. However, it is between the stretches of 500 m and 1,000 m that the greatest accumulations of rubber are observed and, consequently, the lowest measures of friction coefficient.

Still, Chen et al. (2008) also found that the number of landings is directly proportional to the thickness of the rubber deposit in the RWY, where each landing contributes about 0.05 mm to this measurement. This material, when kept in the coating, is subjected to a compaction process due to the weight and heat of the aircraft during landing. As a result, a layer of rubber is formed that occupies the surface of the RWY, making tire-pavement adherence difficult and reducing the friction coefficient in areas with more rubber accumulation.

Flintsch et al. (2005) understand that climate-related factors, such as precipitation, temperature, humidity, wind speed, among others, are partially responsible for seasonal variations in friction properties at the tire-pavement interface. In this case, there are different patterns of seasonal variations in levels of skid resistance; they become more noticeable during the summer months, due to the higher temperatures observed in that season (Masad et al., 2009).

For Masad et al. (2009), friction levels have the lowest values during the summer period. This is due to the greater accumulation of small particles and debris on the pavement surface, which accelerate the polishing of the pavement surface and, consequently, reduce skid resistance. Thus, there is a variation of about 30% of the friction between a minimum in the summer and a peak during the winter (Chelliah et al., 2002).

Anupam et al. (2013) verified the behavior of the friction coefficient regarding the temperature of the pavement, the air and the air inside the tire, in three different types of asphalt mixtures, namely: draining pavement, SMA and thin coating. The results indicate that temperature is inversely proportional to friction, regardless of the type of surface. In addition, the authors developed friction prediction models, using temperature data, through regressions whose Coefficients of Determination (R^2) resulted between 0.81 and 0.94.

3. ARTIFICIAL NEURAL NETWORKS

Artificial Neural Networks (ANN) are computational techniques that portray a mathematical model inspired by the neural structure of intelligent organisms, such as the human brain, and that gain knowledge through experience. In this method, simple processing units are employed that make up distributed parallel systems, called nodes, whose objective is to calculate certain mathematical functions, generally nonlinear. These units are structured in one or more layers, which are interconnected by a significant number of connections (Haykin, 2009).

Haykin (2009) defines a neuron as an information processing unit essential for the functioning of a neural network, that is, the model of a neuron shapes the premise for the design of a large set of neural networks (Figure 1). Thus, three primary components of the neural model are identified, namely: set of synapses or connecting links, sum element and activation function. In the first, each one is defined by its own weight or strength. Notably, multiply a signal xj connected to neuron k at the input of synapse j by the synaptic weight wkj. The importance of recording the way in which the subscripts of the synaptic weight are written is highlighted. The neuron in focus is represented by the first index in wkj, while the end of the synapse input with its respective weight is portrayed by the second. The synaptic weight of an artificial neuron can be found in a range that contains both positive and negative values, as opposed to the weight of a synapse in the brain.

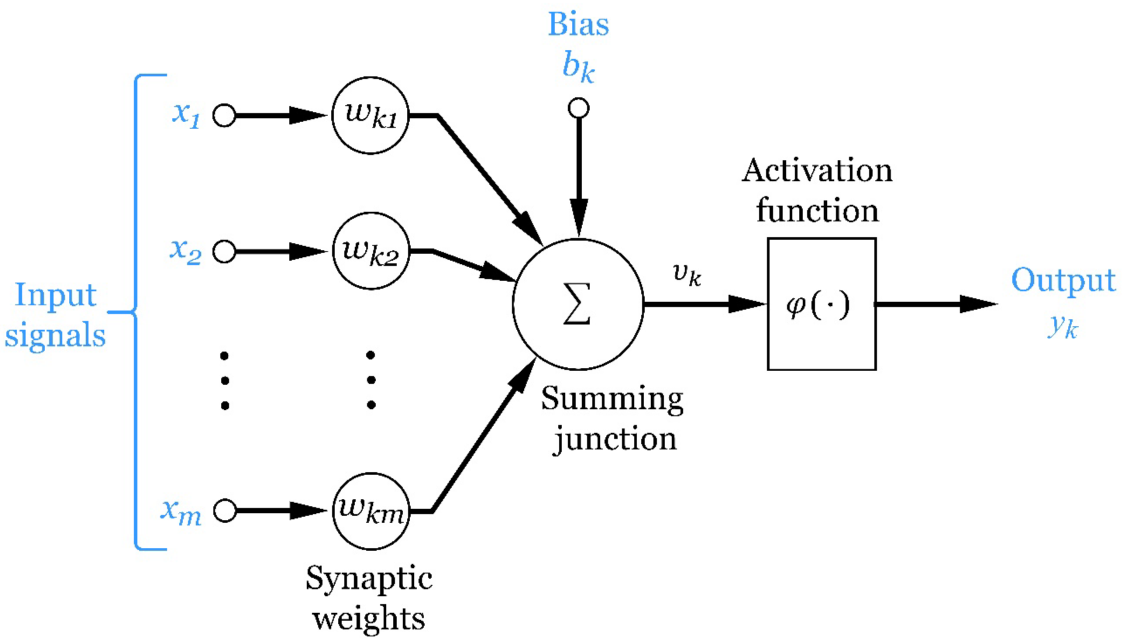

Figure 1. Nonlinear model of a neuron *k*.

The sum element, in turn, performs a sum of the input signals, which are weighted by the respective synaptic weights of the neuron, constituting a linear combination. Finally, the activation function, also known as the squashing function, determines the amplitude of the output of a neuron, in order to limit the allowable amplitude range of the output signal to some finite value (Haykin, 2009).

The normalized amplitude range of a neuron's output typically ranges from $[0, 1]$ or $[-1, 1]$. In addition, the presence of a bias is used externally and has the purpose of changing the activation function of the network, increasing or decreasing it, depending on whether it is positive or negative, respectively (Haykin, 2009). Abiodun et al. (2018) describe that the bias neurons are defined, in any case, as equal to one, in addition to having a similarity with the linear regression interceptor ($y = ax + b$), in which a and b represent, in that order, the coefficient angle of the linear function x and the interceptor.

The Multilayer Perceptron (MLP) consists of a type of neural network similar to the simple Perceptron, but with an undetermined number of neurons present in a set of layers, namely: input layer, one or more hidden or intermediate layers and output layer. In this way, the input signals traverse the network, layer by layer, in a positive direction, that is, from input to output, a movement called feedforward (Bocanegra, 2002).

After the feedforward, the algorithm performs a contrast between the expected value and the value reached by the model, in order to identify errors in the output. Then, the network checks the contribution of each neuron present in the previous intermediate layer to the output error. This process continues until the model reaches the input layer.

According to Géron (2017), the MLP makes a prediction in the input-output direction for each training example through the backpropagation algorithm. In this way, this algorithm runs through each layer in reverse (output-input) to measure the error and verify the contribution of this error for each connection. Finally, the algorithm adjusts the connection weights in order to reduce the error.

When approaching the use of ANN in Transportation Engineering, several authors used this technique to predict parameters related to the condition of tire-pavement adherence, as well as to indicate the need or not for maintenance on the highways and runways (Flintsch et al., 1996; Fwa et al., 1997; Bosurgi and Trifirò, 2005; Thube, 2012; Domitrović et al., 2018; Najafi et al., 2019; Hossain et al., 2019; Ribeiro et al., 2018; Yao et al., 2019; Quariguasi et al., 2021).

4. METHODS

The research method adopted in this study is divided into five stages, namely: choice of aerodrome, data collection, data handling, model development, and analysis and discussion of results.

The chosen aerodromes were two Brazilian international airports, both with flexible pavements in the three RWY (one for Airport A and two for Airport B). The first was selected because of the amount of data provided by the National Civil Aviation Authority (ANAC) and its relevance for air transport in the Northeast region of Brazil in the year 2021 (ANAC, 2021). In turn, the second was defined due to the existence of grooving in one of its RWY and because it is important for air movement in the country.

Variables with precedent in past models applied to highways and airports were used, namely: periodic maintenance (rubber removal), coating age, ambient temperature, relative air humidity and traffic (Fwa et al., 1997; Anupam et al., 2013; Santos et al., 2014; Oliveira, 2017; Susanna et al., 2017; Yao et al., 2019; Quariguasi et al., 2021). In addition, it is noteworthy that, in this work, the existence or not of grooving in the RWY was considered, and that data from the friction coefficient measured by different equipment were used.

Subsequently, data were collected, namely: (i) Friction coefficient measured at 3 m and 6 m on both sides – right/left – of the runway axis; (ii) Longitudinal distance for measuring the friction coefficient in meters; (iii) Side – right/left – of the friction coefficient measurement; (iv) Equipment used to measure the friction coefficient; (v) Date of removal of rubber accumulation; (vi) RWY coating age in months; (vii) Ambient temperature in degrees Celsius; (viii) Relative humidity in percentage; (ix) Existence of grooving; (x) Number of operations (landings and takeoffs).

The data relating to the friction coefficient are as follows: measurement at 3 m and 6 m, measurement distance, measurement side and the equipment used in the test. They were obtained through technical reports provided by ANAC, totaling 22 reports for Airport B and 41 for Airport A, carried out between 2012 and 2018. In addition to these elements, the reports also included the date on which the last rubber accumulation was removed and the existence or not of grooving.

The age of the RWY coating was obtained through the Brazilian Airport Infrastructure Company (Infraero), ANAC and the aerodrome operator of Airport B. For Airport A, the temperature and relative humidity of the air were obtained both through the Airspace Control Institute (ICEA) and through the reports of measurement of the friction coefficient. For Airport B, only these reports were considered as sources for these two variables.

The number of RWY operations was obtained from the websites of ANAC and the airport operator. This information was taken in three different ways, with the aim of representing different scenarios and improving the performance of the models proposed in this work. Thus, the number of RWY operations was analyzed: (i) Between the measurements of the friction coefficient; (ii) By year; (iii) Between rubber buildup removal procedures.

As indicated in the reports adopted in this paper, the friction coefficient referring to Airport A was measured using the GripTester and Skiddometer equipment, both at 65 km/h, whose acceleration distance was 100 m from the predominant threshold. For Airport B, the Mu-Meter equipment was used at the same speed, however, with an acceleration distance of 150 m from the predominant threshold.

The rubber accumulation removal operation was considered only for the first third of the RWY, that is, the initial 900 m and 1,100 m of the predominant threshold for Airports A and B, respectively. This was considered because this segment is the aircraft touchdown zone, where rubber is deposited, especially during landings.

Following the ordering of the data, data pre-processing was performed via Standard Scaler, with the variables mean 0 and variance equal to 1. Pre-processing is a commonly used step in Machine Learning evaluators, aiming to standardize the distributed data for the model not to present unsatisfactory results and for the variables to present a value close to each other, that is, with the same magnitude. Thus, all data are converged to a number close to 0 and have the same order of variation, being contained in the intervals $[0,1]$ or $[-1,1]$.

Subsequently, the data were structured in an $\mathbf{M}\, m \times n$ matrix for insertion in the algorithm. In this matrix, m represents the number of occurrences distributed in lines and n the number of variables separated in columns, including the targets, the friction coefficient measured at 3 m and 6 m, in the last column. Each friction coefficient value (y_1 and y_2) was associated with its respective row of variables (x_{i}).

In the last stage, there is the development of MLP-type ANN models through the Python programming language and its libraries Scikit-learn and Tensorflow. The cross-validation technique was applied, in which the data set was segmented, without repetition and randomly, in a proportion of 80% for training and 20% for testing. R^2 was used to verify the success rate of the algorithm. To verify the error, the Mean Squared Error (MSE) and the Mean Absolute Error (MAE) were used.

5. RESULTS AND DISCUSSIONS

5.1. Results of models AT3 and AT6

The models called Model AT3 and Model AT6, which have the friction coefficient at 3 m and 6 m from the RWY axis as a target variable, were developed using 3,136 instances and 11 classes resulting from a total of 63 measurement reports from Airports A and B. Initially, the following variables were used: measurement distance, measurement side, rubber removal, grooving, equipment used, pavement age, temperature, humidity, number of operations between friction measurements, number of operations between rubber removals, and number of annual operations.

The architecture defined for the models consisted of four hidden layers with 32, 64, 64 and 64 neurons for AT3 and four hidden layers with 64 neurons each for AT6. Both models used the rectified linear activation function and the RMSprop weight optimizer.

Thus, both models were processed five times in order to obtain the average of the results. It is noteworthy that, for each processing, different but close results were obtained. Table 1 shows the test results of the AT3 and AT6 models, using R^2, MSE and MAE.

Table 1: Results of the AT3 and AT6 models

	AT3			AT6		
Runs	**R^2**	**MSE**	**MAE**	**R^2**	**MSE**	**MAE**
1	0.697	0.003	0.043	0.647	0.003	0.044
2	0.699	0.003	0.042	0.649	0.003	0.040
3	0.698	0.003	0.041	0.687	0.003	0.038
4	0.706	0.003	0.043	0.674	0.003	0.038
5	0.717	0.003	0.042	0.700	0.002	0.036
Average	0.703	0.003	0.042	0.671	0.003	0.039

It is verified, through Table 1, that the R^2 of the models resulted in values around 0.70, which represents a satisfactory value given the complexity of the problem. The MSE resulted in 0.003 and the MAE was around 0.040 for both models. It is also noticed that the R^2 and the MAE presented, respectively, an increasing and decreasing value, according to the processing order for both the AT3 and AT6 models. However, this improvement observed in the result has no correlation with the order or amount of processing.

It is noteworthy that the results of the models are different at each processing due to the cross-validation procedure, which consists of randomly dividing the data set into k exclusive partitions. In this case, a subset is used for testing and the rest for training for each partition, alternately, that is, for each processing, the model is processed and tested with a different partition of the data. Figure 2 shows the scatter plot between the observed and estimated friction coefficient in the test phase of the AT3 and AT6 models.

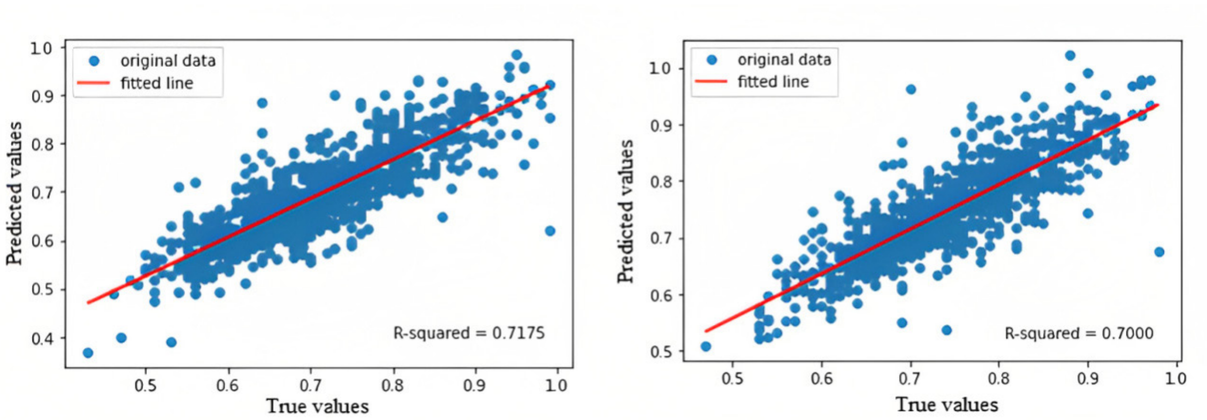

Figure 2. AT3 and AT6 model test scatter plot.

It can be seen from Figure 2 that the results of the models were satisfactory in generalizing the problem. This is because the values are close to the diagonal that represents the trend line, showing a positive correlation between the observed and the estimated friction coefficient. Despite the dispersion of some points, it can be seen that, in the best processing result, the AT3 and AT6 models exhibited an R^2 of 0.72 and 0.70, respectively. Regarding the worst result, the models presented an R^2 of 0.70 and 0.65.

5.2. Results of models AT3 and AT6 with change of variables

The analysis of the results resulting from the alteration of the input variables of Models AT3 and AT6, in which two modifications were performed with the objective of improving accuracy, is presented in this item. It is noteworthy that the architectures of the models were not changed, that is, four hidden layers with 32, 64, 64 and 64 neurons for AT3 and four hidden layers with 64 neurons each for AT6.

In the first modification, the following variables were removed: pavement age, operations between rubber removals, and annual operations. In the second change, the grooving variable was removed, in addition to those removed first. The pavement age variable was removed due to its low correlation coefficient with the friction coefficient at 3 m and 6 m, presenting values of 0.10 and 0.07, respectively. Furthermore, the data showed high dispersion and a coefficient of variation of 0.74, which may reduce the accuracy of the model. It should be noted that this variation was due to the average RWY resurfacing interval of 120 months.

As for the variables related to the number of operations, only one of the three variables was used in the first processing in order to reduce the redundancy of this type of data. The two variables removed were chosen because they have a lower coefficient correlation with the friction coefficient. The grooving variable was dispensed due to its smaller number of instances in relation to the data set.

Two distinct results were obtained for each model relative to the first and second changes made. That said, four new models were named for better interpretation, namely: Models AT3-1, AT3-2, AT6-1, AT6-2. It is assumed that the altered models presented similar results to the first processing (Table 2).

Table 2: Results of AT3 model with change of variables

	AT3-1 (1st change)			**AT3-2 (2nd change)**		
Runs	**R^2**	**MSE**	**MAE**	**R^2**	**MSE**	**MAE**
1	0.697	0.003	0.044	0.680	0.003	0.045
2	0.714	0.003	0.041	0.663	0.004	0.046
3	0.707	0.003	0.041	0.680	0.004	0.045
4	0.715	0.004	0.046	0.692	0.003	0.043
5	0.704	0.003	0.042	0.708	0.003	0.043
Average	0.707	0.003	0.043	0.685	0.003	0.044
AT3 Results	0.703	0.003	0.042	-	-	-

The AT3-1 and AT3-2 models showed an average R^2 of 0.707 and 0.685, respectively, in addition to an MSE of 0.003 and a MAE of 0.044. In comparison with the R^2 of 0.703, of the AT3 model, it is verified that the removal of the variables pavement age, operations between rubber removals and annual operations improved the performance of the model, while the elimination of the grooving variable reduced the accuracy, as illustrated in Table 2.

Models AT6-1 and AT6-2 presented an average R^2 of 0.619 and 0.633 and a MAE of 0.043 and 0.040, respectively, in addition to an MSE of 0.003 in both (Table 3). The results of the two changes made were lower than those obtained in the AT6 model, that is, the model obtained better accuracy and generalization using all available data. The R^2 had a reduction from 0.671 to 0.619 in the first modification and to 0.633 in the second modification, in which the removal of the grooving variable increased the accuracy of the model in relation to the first modification. This may be associated with the smaller amount of data that has the grooving variable in relation to the dataset.

Table 3: Results of AT6 model with change of variables

	AT6-1 (1st change)			**AT6-2 (2nd change)**		
Runs	**R^2**	**MSE**	**MAE**	**R^2**	**MSE**	**MAE**
1	0.563	0.004	0.045	0.599	0.003	0.043
2	0.603	0.004	0.048	0.623	0.003	0.041
3	0.634	0.003	0.044	0.648	0.003	0.040
4	0.642	0.003	0.040	0.648	0.003	0.038
5	0.651	0.003	0.038	0.646	0.003	0.038
Average	0.619	0.003	0.043	0.633	0.003	0.040
AT6 Results	0.671	0.003	0.039	-	-	-

Although the changes in the variables did not promote a significant improvement in the accuracy of the models, the number of variables and data needed to obtain a result close to those of the AT3 and AT6 models, which encompass all the variables, was reduced. In this way, the effort required to collect and store data was reduced, as well as the financial expenditure for these activities. In a possible application of these models, cost reduction for the aerodrome operator is an important factor for the implementation and maintenance of such systems.

In addition, carrying out measurements of the friction coefficient of RWY represents a financial, personnel and logistical effort for the aerodrome operator, requiring the RWY to be closed for such activities. Therefore, the application of models that can reduce the number of measurements carried out on the runway and, consequently, the costs linked to these activities, is useful for aerodrome operators in relation to the management of airport pavements and for ANAC in terms of inspection and regulation of national civic aviation.

Finally, it can be understood that there was an improvement in the models, since the number of variables was reduced, maintaining an accuracy close to that observed in the models according to all available data. Indeed, the reduction of the database without harming the accuracy represents an improvement in the models.

5.3. Grooving influence

The statistical analysis of the relationship between grooving and the friction coefficient measured at 3 m and 6 m from the RWY axis is addressed in this item. Initially, descriptive statistics were performed on the data, dividing the occurrences by the distance from the axis and the presence of grooving (Table 4).

Table 4: Descriptive statistics of the friction coefficient in relation to grooving

Variable	Data	Mean	Standard Deviation	Coefficient of Variation	Minimum	Maximum
Friction coefficient at 3 m	All	0.71	0.10	0.14	0.38	0.99
	No grooving	0.73	0.10	0.14	0.38	0.99
	With grooving	0.65	0.06	0.10	0.48	0.83
Friction coefficient at 6 m	All	0.75	0.09	0.12	0.47	0.99
	No grooving	0.76	0.09	0.11	0.47	0.99
	With grooving	0.69	0.07	0.10	0.50	0.87

It can be seen that the average friction coefficient observed in measurements with grooving showed lower averages compared to measurements without the device (Table 4). In addition, the maximum and minimum values of the friction coefficient were verified in the measurements without grooving. It should be noted that the measurements of the entire length of the RWY of the two aerodromes analyzed were used and that only the runway 11L/29R has grooving.

Through an analysis of the distribution of occurrences, it can be seen that the coefficients of friction measured at 3 m and 6 m are higher in areas without grooving (Figures 3 and 4). It is also noted that the measurements taken at 6 m are larger than the measurements at 3 m. This may be associated with the number of operations per size of aircraft; large aircraft influence more at 6 m from the RWY axis due to the width of their landing gear and wear out that region of the RWY more when compared to small and medium-sized aircraft that operate in the 3 m range.

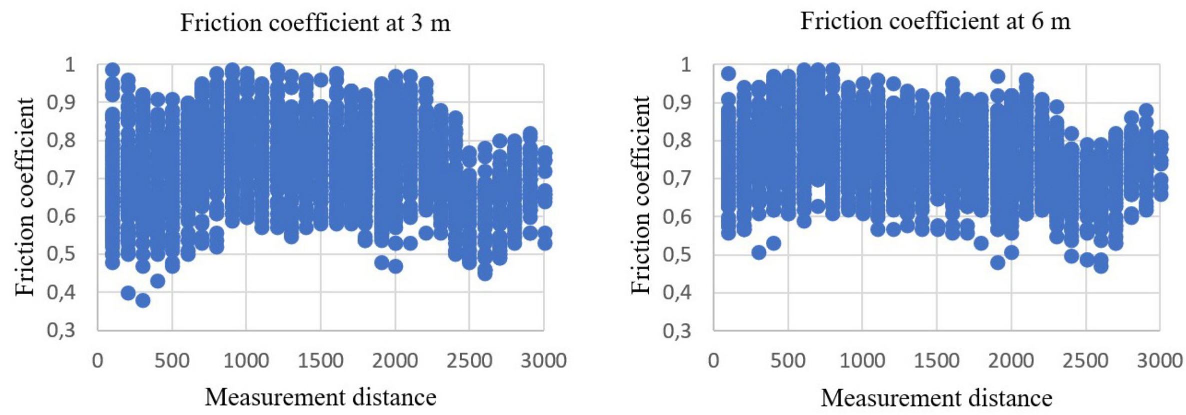

Figure 3. Scatter plots of friction coefficient according to measurement distance in RWY without grooving.

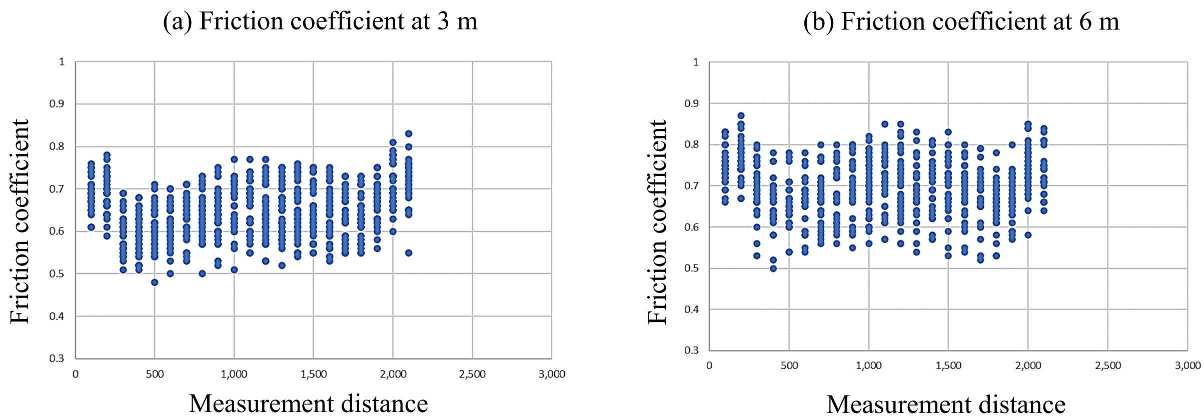

Figure 4. Scatter plots of friction coefficient according to measurement distance in RWY with grooving.

The fact that the areas with grooving have the lowest friction coefficient measures may be related to the aircraft touchdown zone, located in the 1st third of the RWY and where takeoff and landing operations are performed. These areas tend to have more rubber build-up that tends to fill in the existing grooves and, in turn, a reduction in the friction coefficient.

It can be understood that the effectiveness of grooving decreases as operations in the RWY are performed and the residue is deposited in the grooves. Therefore, the rubber removal procedure is important precisely to return the friction coefficient to its initial value. However, these interventions may not be carried out at the right time, so as not to remove the rubber accumulation and reduce the friction coefficient measurements.

Finally, the installation of grooving is recommended to improve the friction coefficient of the PPD. However, the functionality of the device is directly related to carrying out maintenance by removing the rubber in an appropriate period.

6. CONCLUSIONS

This research developed and improved prediction models for the friction coefficient measured by different equipment at 3 m and 6 m away from the runway (RWY) axis, using Artificial Neural Networks (ANN). Thus, the models developed showed satisfactory results, with a hit rate of around 0.70, which validate their possibility of use to obtain estimates of the friction coefficient.

In addition, the results of the models showed the viability of using friction coefficient data measured by different equipment in ANN models. Although the models need improvement to develop their accuracy, it is understood that they can have better results from a quantitatively larger database and with a greater number of aerodromes.

The results obtained resulting from the alterations, with *x* variables, were similar to the initial processing, in which all *y* variables were used. The accuracy of the altered models was lower, but close to that of the initial model. Although the accuracy was not increased by changing the variables, it can be considered an adequate result, since a result similar to that of the first processing was achieved, using a smaller amount of data. It is emphasized that the need for a smaller database represents an improvement of the models, in view of the limitation in obtaining data for carrying out this research.

Regarding the grooving analysis, it was found that the measurements that had this device had lower averages in relation to the others. It was verified that this result may be associated with the location of the grooving in the RWY, that is, the touchdown zones of the aircraft tend to have a lower friction coefficient due to the accumulation of rubber. Moreover, failure to remove this accumulation in an appropriate period may have also contributed to a greater amount of accumulated rubber and, consequently, a lower friction coefficient.

Regarding the limitations of this research, the models were developed only with data from the Brazilian international airports and, therefore, may not be appropriate for other airfields with different characteristics. In addition to that, only one RWY showed grooving, that is, there was a greater amount of data for measurements without the device. The prediction models were developed for the friction coefficient measured at 3 m and 6 m away from the RWY axis with the GripTester, Skiddometer and Mu-Meter equipment at 65 km/h such that the models could present inconsistency in different scenarios of these circumstances. Still, the use of variables that extrapolate the values used for training the models can also cause errors.

Finally, it is evident that this research contributes to the increase of operational safety in Brazilian RWY and with the pavements management system by the aerodrome operator regarding the condition of tire-pavement adherence. Furthermore, this paper can also help in ANAC's inspection and regulation activities.

ACKNOWLEDGEMENTS

This work was carried out with the support of the Coordination for the Improvement of Higher Education Personnel – Brazil (CAPES) – Financing Code 001. To the Department of Airport Infrastructure of the National Civil Aviation Authority for providing the data.

REFERENCES

Abiodun, O.I.; A. Jantan; A.E. Omolara et al. (2018) State-of-the-art in artificial neural network applications: a survey. *Heliyon*, v. 4, n. 11, p. E00938. DOI: 10.1016/j.heliyon.2018.e00938.

ANAC (2019) RBAC 153: Aeródromos - Operação, Manutenção e Resposta à Emergência. Emenda nº 4. Brasília: Agência Nacional de Aviação Civil.

ANAC (2021) Consulta Interativa – Indicadores do Mercado de Transporte Aéreo. Brasília: Agência Nacional de Aviação Civil.

Anupam, K.; S.K. Srirangam; A. Scarpas et al. (2013) Influence of temperature on tire-pavement friction analyses. *Transportation Research Record*, v. 2369, n. 1, p. 114-124. DOI: 10.3141/2369-13.

Aps, M. (2006) *Classificação da Aderência Pneu-Pavimento Pelo Índice Combinado IFI – International Friction Index para Revestimentos Asfálticos*. Thesis (Ph.D.). Escola Politécnica, Universidade de São Paulo, São Paulo, SP. DOI: 10.11606/T.3.2006.tde-11122006-144825

Bocanegra, C.W.R. (2002) *Procedimentos para Tornar Mais Efetivo o Uso das Redes Neurais Artificiais em Planejamento de Transportes*. Dissertation (master of science). Escola de Engenharia de São Carlos, Universidade de São Paulo, São Carlos, SP. DOI: 10.11606/D.18.2002.tde-06032002-131951.

Bosurgi, G. and F. Trifirò (2005) A model based on artificial neural networks and genetic algorithms for pavement maintenance management. *International Journal of Pavement Engineering*, v. 6, n. 3, p. 201-209. DOI: 10.1080/10298430500195432.

Chelliah, T.; P. Stephanos; T. Smith et al. (2002) Developing a design policy to improve pavement surface characteristics. In Transportation Research Board (ed.) *Pavement Evaluation Conference*. Location: Transportation Research Board, p. 1-19.

Chen, J.S.; C.C. Huang; C.H. Chen et al. (2008) Effect of rubber deposits on runway pavement friction characteristics. *Transportation Research Record*, v. 2068, n. 1, p. 119-125. DOI: 10.3141/2068-13.

Costa, S.L.; V.T.F. Castelo Branco and E.F. Freitas (2017) *Avaliação da aderência pneu-pavimento para diferentes tipos de pavimentos utilizando o International Friction Index (IFI)*. In Associação Nacional de Pesquisa e Ensino em Transporte (org.) *XXXI Congresso da Associação Nacional de Pesquisa e Ensino em Transporte*. Recife: ANPET, p. 1-12.

Domitrovic, J.; T. Rukavina and H. Dragovan (2018) Application of an artificial neural network in pavement management system. *Technical Gazette*, v. 25, p. 466-473. DOI: 10.17559/TV-20150608121810.

Flintsch, G.W.; J.P. Zaniewski and J. Delton (1996) Artificial neural network for selecting pavement rehabilitation projects. *Transportation Research Record*, v. 1524, n. 1, p. 185-193. DOI: 10.1177/0361198196152400122.

Flintsch, G.W.; Y. Luo and I.L. Al-Qadi (2005) Analysis of the effect of pavement temperature on the frictional properties of flexible pavement surfaces. In Transportation Research Board (org.) *84th Transportation Research Board Annual Meeting*. Washington, D.C.: Transportation Research Board.

Fonseca, O.A. (1990) *Manutenção de Pavimentos de Aeroportos*. Brasília: Diretoria de Engenharia da Aeronáutica/Divisão de Estudos e Projetos de Infraestrutura/Ministério da Aeronáutica.

Fwa, T.F.; W.T. Chan and C.T. Lim (1997) Decision framework for pavement friction management of airport runways. *Journal of Transportation Engineering*, v. 123, n. 6, p. 429-435. DOI: 10.1061/(ASCE)0733-947X(1997)123:6(429).

Géron, A. (2017) *Hands-on Machine Learning with Scikit-learn & TensorFlow*. Sebastopol: O'Reilly.

Haykin, S. (2009) *Neural Networks and Learning Machines* (3rd ed.). Upper Saddle River, NJ: Pearson.

Hossain, M.I.; L.S.P. Gopisetti and M.S. Miah (2019) International roughness index prediction of flexible pavements using neural networks. *Journal of Transportation Engineering, Part B: Pavements*, v. 145, n. 1, p. 04018058. DOI: 10.1061/JPEODX.0000088.

ICAO (2019) *State of Global Aviation Safety: Safety Report*. Montreal: International Civil Aviation Organization.

Kazda, A. and R.E. Caves (2007) *Airport Design and Operation* (2nd ed). New York: Elsevier Science.

Masad, E.; A. Rezaei; A. Chowdhury et al. (2009) *Predicting Asphalt Mixture Skid Resistance Based on Aggregate Characteristics*. Austin: Texas Transportation Institute. Available at: <https://static.tti.tamu.edu/tti.tamu.edu/documents/0-5627-1.pdf > (accessed 03/17/2023).

McDaniel, R.S.; K.J. Kowalski; A. Shah et al. (2010) *Long Term Performance of a Porous Friction Course*. West Lafayette: Taylor & Francis Online.

Najafi, S.; G.W. Flintsch and S. Khaleghian (2019) Pavement friction management – artificial neural network approach. *International Journal of Pavement Engineering*, v. 20, n. 2, p. 125-135. DOI: 10.1080/10298436.2016.1264221.

Oliveira, P.V.S. (2017) *Estudo Preliminar do Comportamento da Capacidade de Atrito nas Pistas de Pouso e Decolagem do Aeroporto Pinto Martins*. Undergraduate thesis (bachelor degree). Universidade Federal do Ceará, Fortaleza, CE. Available at: <http://www.repositorio.ufc.br/handle/riufc/29491> (accessed 03/17/2023).

Quariguasi, J.B.F.; F.H.L. Oliveira and S.D.S. Reis (2021) A prediction model of the coefficient of friction for runway using artificial neural networks. *Transportes*, v. 29, n. 2, p. 2401. DOI: 10.14295/transportes.v29i2.2401.

Ribeiro, A.J.A.; C.A.U. Silva and S.H.D.A. Barroso (2018) Metodologia de baixo custo para mapeamento geoté cnico aplicado à pavimentação. *Transportes*, v. 26, n. 2, p. 84-100. DOI: 10.14295/transportes.v26i2.1491.

Santos, A.; E. Freitas; S. Faria et al. (2014) Degradation prediction model for friction in highways. In Murgante, B.; S. Misra; A.M.A.C. Rocha et al. (eds.) *Computational Science and Its Applications - ICCSA 2014 14th International Conference, Guimarães, Portugal, June 30 - July 3, 204, Proceedings, Part III.* Cham: Springer, p. 606-614. DOI: 10.1007/978-3-319-09150-1_44.

Shahin, M.Y. (2005) *Pavement Management for Airports, Roads, and Parking Lots* (2nd ed). New York: Springer.

Skerritt, W.H. (1993) Aggregate type and traffic volume as controlling factors in bituminous pavement friction. *Transportation Research Record*, v. 1418, p. 22-29.

Susanna, A.; M. Crispino; F. Giustozzi et al. (2017) Deterioration trends of asphalt pavement friction and roughness from medium-term surveys on major Italian roads. *International Journal of Pavement Research and Technology*, v. 10, n. 5, p. 421-433. DOI: 10.1016/j.ijprt.2017.07.002.

Thube, D.T. (2012) Artificial Neural Network (ANN) based pavement deterioration models for low volume roads in India. *International Journal of Pavement Research and Technology*, v. 5, n. 2, p. 115-120.

Yao, L.; Q. Dong; J. Jiang et al. (2019) Establishment of prediction models of asphalt pavement performance based on a novel data calibration method and neural network. *Transportation Research Record*, v. 2673, n. 1, p. 66-82. DOI: 10.1177/0361198118822501.